Imaging Modalities Employed in the TAVR Procedure With a Focus on CTA: What the Radiologist Needs to Know

Lina Karout, MD, Rida Salman, MD, Firas Ershaid, MD, Fadi Sawaya, MD, Alain S. Abi-Ghanem, MD

Rationale and Objectives: Aortic stenosis (AS) is one of the most common valvular heart disease. Symptomatic AS is associated with a high mortality rate which prompts fast intervention. The introduction of transcatheter aortic valve replacement (TAVR) has drastically improved the outcome of high surgical risk for mortality patients with severe AS. However, this procedure requires the employment of multimodality imaging in the pre-procedural planning, intra-procedural optimization, and post-procedural follow-up stages. This also requires an accurate understanding of the indications, measurements, strength, and limitations of each imaging modality during the different TAVR stages.

Conclusion: In this review, we aim to outline to radiologists the evidence-based approach and indications of different imaging modalities through the pre, peri, and post TAVR stages.

KEY WORDS: Transcatheter Aortic Valve Implantation; CT Angiography; Transthoracic Echocardiography; Transesophageal Echocardiography.

Abbreviations: AS Aortic stenosis, **TAVR** Transcatheter aortic valve replacement, **SAVR** Surgical aortic valve replacement, **CTA** Computed tomography angiography, **TEE** Transesophageal echocardiography, **CT** Computed tomography, **TTE** Transthoracic echocardiography, **AVA** Aortic valve opening area, **LV** Left ventricle, **LVOT** Left ventricular outflow tract, **CMR** Cardiovascular Magnetic Resonance, **MRA** Magnetic Resonance Angiography, **SSFP** Steady-state free precession, **BAV** Bicuspid aortic valve, **STJ** Sinotubular junction, **AR** Aortic regurgitation, **MR** Mitral regurgitation, **BASILICA** Bioprosthetic or native aortic scallop intentional laceration to prevent iatrogenic coronary artery obstruction, **EOA** Effective orifice area, **CCT** Cardiac computed tomography, **HALT** Hypoattenuated Leaflet Thickening, **RLM** Reduced Leaflet Motion, **PDIP-SOS** Proton density-weighted in-phase stack of stars.

INTRODUCTION

Aortic stenosis (AS) is one of the most common type of valvular heart disease (1, 2). The prevalence of moderate AS can be as high as 5% in 75-year-old patients (3). Symptomatic AS is associated with a high mortality rate which prompts fast surgical aortic valve replacement (SAVR) or transcatheter aortic valve replacement (TAVR) to alleviate the stenotic valve and improve survival (4). TAVR is a minimally invasive procedure that has drastically improved the outcome of patients with severe aortic valve disease (1, 4). Procedure-related complications are majorly related to inaccurate image assessment of multiple significant parameters as annular geometry (1). Multi-image modalities are employed during TAVR planning, TAVR procedure, and follow-up. Echocardiography is used as the first image modality to assess and diagnose AS and establish its severity (5). However, computed tomography angiography (CTA) is the gold standard study for planning, guiding TAVR procedure, and predicting risks and possible complications. CTA helps to improve the clinical outcome of patients with AS by adequate patient selection, treatment planning, device selection, and positioning (6). In this review, we aim to highlight from a radiologist's point of view the multitude of image modalities employed pre, peri, and post-TAVR procedures with an increased focus on CTA.

PRE-TAVR IMAGING

Table 1 provides a summary of the parameters to be assessed with the respective image modalities employed in the pre-TAVI stage.

Acad Radiol 2022; 29:S69–S81

From the Department of Radiology, American University of Beirut Medical Center, Lebanon. P.O.Box: 11-0236 Riad El-Solh, Beirut, 1107 2020, Lebanon (L.K., F.E., A.S.A.-G.); Edward B. Singleton Department of Radiology, Texas Children's Hospital and Baylor College of Medicine, 6701 Fannin St., Suite 470, Houston, TX 77030 (R.S.); Department of Cardiology, American University of Beirut Medical Center, Lebanon. P.O.Box: 11-0236 Riad El-Solh, Beirut, 1107 2020, Lebanon (F.S.). Received May 30, 2021; revised August 10, 2021; accepted August 11, 2021. **Address correspondence to:** A.A. e-mail: aa277@aub.edu.lb

https://doi.org/10.1016/j.acra.2021.08.012

TABLE 1. Summary of the parameters to be assessed in the pre-TAVI stage.

	Parameters	Image Modality	Importance and Complication(s)
Aortic Valve Complex	Aortic Annulus	Can be assessed by echocardiography, ECG-synchronized CTA and MRA. ECG-synchronized CTA is the image modality of choice. TEE is employed when CTA is contraindicated.	Important parameter used to determine prosthetic valve sizing. Oversizing may result in annular rupture. Under sizing may result in paravalvular regurgitation.
	Valvular and device landing zone calcification	Can be assessed qualitatively by echocardiography, and quantitatively and qualitatively by CT and MRI.	Important to be assessed since it affects AS severity. Severe aortic stenosis is very likely when CT Agatston scores are $\geq$ 3000 for men and $\geq$ 1600 for women. Severe calcifications in LVOT increase the risk of complications. Severe calcifications in the landing zone and in the aortic valve increase the risk of paravalvular regurgitation and rupture.
	Aortic Valve Cuspidity	Can be assessed by echocardiography, CT and MRI. TEE and CT are preferred in severely calcified valve.	Important to classify aortic valve. Ascending aortic dilation and aneurysms are more commonly seen in the bicommissural morphology.
	Coronary ostial height and sinus of valsalva	CT	Coronary ostial height is important to be measured since short heights are associated with periprocedural coronary occlusion.
	Sinotubular Junction	CT	STJ diameter smaller than the transcatheter heart valve predicts a higher risk of STJ injury in the case of balloon-expandable devices.
Aortic Stenosis Severity	Aortic Valve opening Area (AVA). AVA indexed to body surface area. Aortic Jet Velocity Transaortic Gradient Pressure	Echocardiography AVA can be measured by CCT and CMR when echocardiography is equivocal.	Important parameters measured by transthoracic echocardiography to classify and assess aortic valve severity.
Vascular Access Planning	Assess the arterial caliber Assess the vascular angulation Assess for the presence of calcification Assess vascular tortuosity Assess the atherosclerotic burden	Non-ECG synchronized CTA or unenhanced MRI CTA is the gold standard image modality for assessment of vascular access. Unenhanced CMR is used when CTA is contraindicated. Duplex ultrasound is used in transcarotid approach	

Diagnosis of Aortic Stenosis

Echocardiography: is the first image modality employed to diagnose AS. It plays an essential role in TAVR planning since it confirms the presence of severe AS disease and provides additional anatomical and functional information which is crucial in this stage. Echocardiography enables the visualization of the morphology, number, and movement of aortic cusps. In addition, it helps to qualitatively assess the presence of calcium deposition (7). It is worth noting that in severely calcified aortic valves, 2D transthoracic echocardiography (TTE) should be substituted by transesophageal echocardiography (TEE) or computed tomography (CT) scan since they provide better and accurate visualization of aortic valve morphology which is essential for estimating the prosthetic valve sizing (7). Therefore, TEE is considered the gold standard modality for AS assessment since it overcomes TTE limitations such as poor acoustic window and provides better visualization of aortic valve morphology when calcified AS is present (5). Due to its more invasive nature, TEE is employed when there is uncertainty of the AS diagnosis, aortic calcification, or limited sonographic window of imaging during TTE (8).

The flow-dependent aortic jet velocity and transaortic gradient pressure and the flow-independent aortic valve opening area (AVA) are key parameters used in the diagnosis of severe AS (9). Almost 50% of severe AS present as a high gradient. The other 50% consists of low flow or/and low gradient AS. According to the 2014 American Heart Association and American College of Cardiology Valvular heart disease guidelines, and in the setting of normal stroke volume, severe high gradient AS is defined by the presence of aortic transvalvular velocity of $\geq$ 4 m/s and/or mean transvalvular gradient pressure $\geq$ 40 mm Hg and AVA $\leq$ 1 cm2 or AVA index $\leq$ 0.6 cm2/m2. Low flow AS is defined as AVA $\leq$ 1 cm2 (with AVA indexed to body surface area $\leq$0.6 cm2/m2) and stroke volume $\leq$ 35 mL/m2. Low gradient AS is defined as AVA $\leq$ 1 cm2 (with AVA indexed to body surface area $\leq$0.6 cm2/m2) with a gradient pressure < 40 mmHg (10).

Patients with low gradient severe AS can have true severe or pseudo-severe AS (low transvalvular gradient is caused by mild/moderate AS with low stroke volume mimicking severe AS). Pseudo-severe AS are unlikely to benefit from TAVR; therefore, it is essential to differentiate between these entities by dobutamine echocardiography. Low dose dobutamine (20 μg/kg/min) induces an increase in left ventricle (LV) contraction resulting in a constant AVA <1 cm2 with an increased mean gradient in true severe AS and failure to increase in pseudo-severe AS (7). Figure 1 demonstrates the transthoracic echocardiographic algorithmic approach in the diagnosis and assessment of severe aortic stenosis.

High attention should be taken when calculating the following parameters:

- The aortic jet velocity is the peak velocity measured by continuous-wave doppler US at any window. Radiologists should measure the highest velocity multiple times in different windows to obtain accurate values (9). A study of 100 consecutive patients with severe AS shows that measuring the highest velocity in the right parasternal window was superior compared with other windows. On contrary,

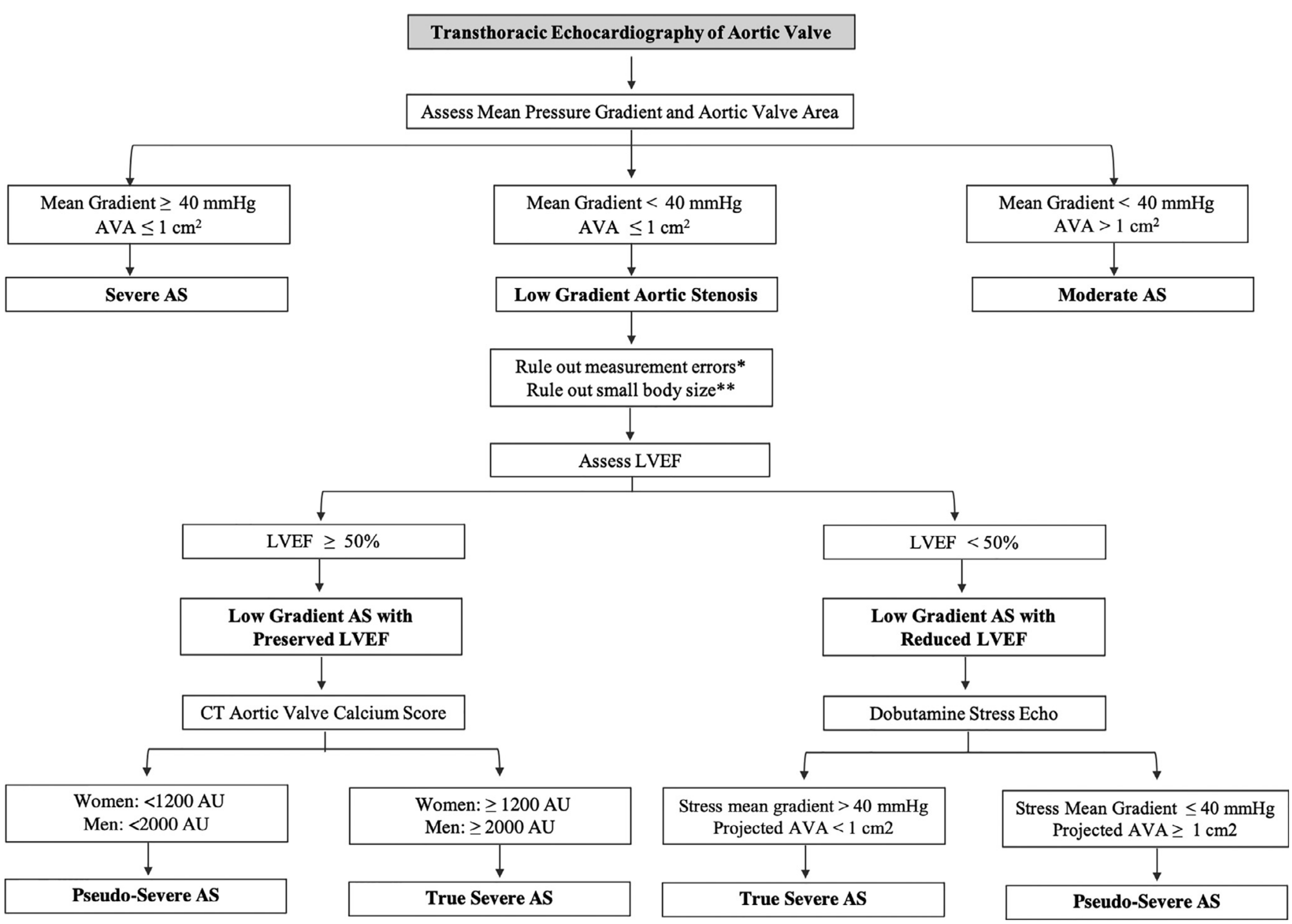

Figure 1. Transthoracic echocardiographic approach for the diagnosis of aortic stenosis. *Calculate doppler velocity (<0.25), Corroborate measurement of LVOT diameter by 3D TTE/TEE, LVOT stroke volume by other echo methods and measurement of AVA by other echo methods. ** Calculate indexed AVA (<0.6 cm2/m2).

the measurement of the highest velocity in the apical window was associated with the misclassification of AS (11).

- The left ventricular outflow tract (LVOT) diameter is one of the parameters used to calculate the AVA. It should be measured in the mid-systole phase of the cardiac cycle in-between the inner edges approximately 0.5-1 cm below the aortic annulus. Calcification in this area should be excluded to avoid underestimation of LVOT which consequently will underestimate the severity of AS (12). 3D-TTE is preferred in measuring LVOT since it reveals its elliptical shape and avoids inaccurate measurements when compared to 2D TTE (11).

Echocardiography is known for its limitations (5):

- It is an operator-dependent image modality; hence, we only recommend experienced operators to assess AS in this setting.
- It has poor acoustic windows and lacks a three-dimensional image aspect.
- Inadequate alignment of the ultrasound beam and flow dependence could result in inaccurate measurements.

Computed tomography (CT) and Cardiovascular Magnetic Resonance (CMR)

CT may be beneficial to refine AS diagnosis where it allows the measurement of the AVA (13), the assessment of aortic valve cuspidity when echocardiography is equivocal (14, 15), and the evaluation of valvular and landing zone calcifications (16). Aortic valve calcification with cardiac computed tomography (CCT) is highly reproducible (17). It can be quantified by the employment of the Agatston score with non-contrast CCT. Clavel *et al.* showed a correlation between aortic valve calcium score and AS severity which made the use of non-contrast CCT important in patients with unknown severity (18). The technique is similar to the one used in coronary artery calcium score evaluation with sex-specific thresholds; an Agatston score of $\geq$3,000 in men and $\geq$1,600 in women predicts severe AS, while an Agatston score of <1,600 in men and <800 in women indicates a less probability of severe stenosis (16). CMR can be used to evaluate AS severity anatomically by assessing valve planimetry using high-resolution steady-state free precession (SSFP) cine images (19). Furthermore, it allows the evaluation of aortic valve cuspidity when echocardiography is equivocal (15).

AORTIC VALVE COMPLEX AND MEASUREMENTS

The aortic root consists of aortic valve cusps and its leaflet attachments, the fibrous interleaflet triangles, sinotubular junction, sinuses of Valsalva, and the annulus (Fig 2a) (20, 21). One of the most important steps in planning for TAVR is the measurement of aortic valve dimensions which include the LVOT, aortic root components, and height of coronary arteries. Those factors are essential to determine the appropriate size of the prosthetic valve and subsequently prevent the prevalence of peri and post TAVR complications (11). For example, over or under-sizing of TAVR prosthesis may result in aortic root rupture, valve embolization, or paravalvular regurgitation (7).

Aortic Annulus

The aortic annulus is the most important parameter used to determine prosthetic valve sizing (11). It is an asymmetrical oval and virtual ring formed by the basal hinge point of the aortic valve cusps (Fig 2b). This results in the shortest annulus measurement when imaged at the sagittal plane and the longest measurement in the coronal plane (11). 3D image modalities are preferred over 2D in visualizing the annulus due to their elliptical nature. The annulus is measured at the lowest hinge point of the aortic leaflets of the aortic root at mid-systole at the sagittal plane parasternal for TTE and mid-esophagus for TEE. TEE can be used for the assessment of AS severity when there is uncertainty of diagnosis or limited window when employing TTE. By employing TEE, deep gastric views, Aortic valve gradient and PW doppler of LVOT can be easily obtained. Interestingly, studies have shown that the 3D TEE aortic annular sizing measurements correlate well with CT measurements. Therefore, 3D multiplane TEE is the imaging modality of choice to measure aortic annular sizing when CT is contraindicated (8).

Computed Tomography

CT is the imaging technique of choice in evaluating aortic valve anatomy and size. It provides an accurate assessment of aortic root, aortic valve, commissures, annulus, calcifications, and distance from coronary ostia (5).

ECG-synchronized CTA of the aortic root and heart: during the entire cardiac cycle should be obtained since aortic root parameters differ throughout the cardiac cycle. Systolic scan coverage, during which the largest aortic root dimensions are obtained, is needed to choose the adequate size of the transcatheter heart valve (22, 23). Diastolic scan coverage assesses the aortic valve morphology and plays a major role in the determination of valve size in the case of septal hypertrophy (23-25). The axial thin-sliced multiphasic data set should be obtained with <1mm slice thickness, small field of view, and a 512 × 512 matrix for ECG-synchronized CTA of the aortic root and heart in order to cover the cardiac structures alone and to have a better spatial resolution. Furthermore, the mean age of patients treated with TAVR is around 80 years old in multiple clinical trials (26, 27). Thus, the image quality, rather than radiation dose, will be the major concern during image acquisition, to avoid study repetition and contrast administration, specifically in this age group which is more prone to kidney dysfunction.

An adequate arterial opacification (>250 HU) is needed after contrast administration (28) for better vascular evaluation. The administered contrast dose is usually between 50

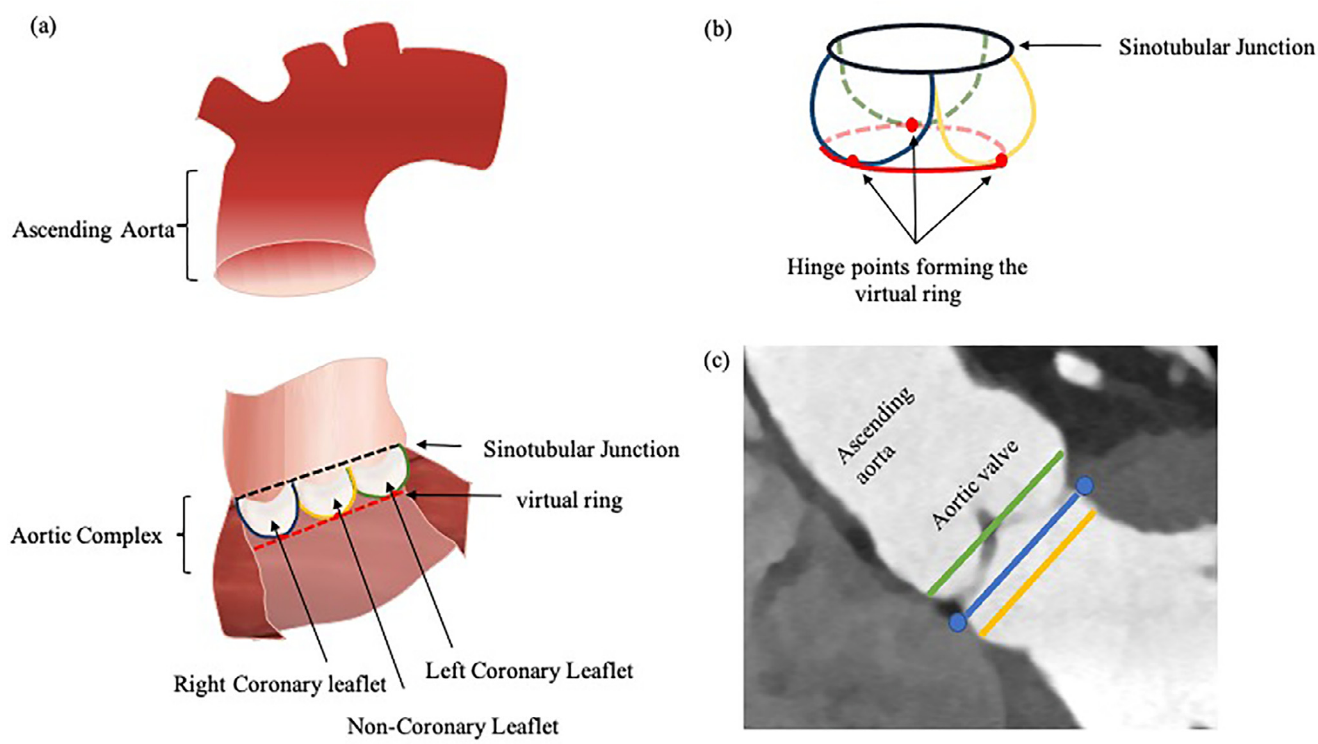

Figure 2. illustrates a schematic drawing of the (a) ascending aorta and its corresponding aortic complex, (b) the three-dimensional crown-like arranged aortic root showing the left, right, and noncoronary cusps and their corresponding hinge points forming the virtual annular ring (red ring) and (c) the axial CT image of the aortic complex showing the true measurement at the level of the virtual ring (blue line), measurement at the level of the upper outflow tract with good correlation with hinge point plane (yellow line) and measurement upward in the aortic sinus overestimating annulus size (green line).

and 100 cc, with lower doses in case of kidney dysfunction. Image quality can be affected by elevated heart rate. However, heart rate control with beta-blockers is not advised due to its side effects in case of severe aortic stenosis (6).

Aortic annulus definitions and measurement techniques: The transection of the most basal attachment points of the three aortic valve cusps in one plane is essential for anatomical sizing of the aortic annulus. The annular plane can be identified manually by standard multiplanar reformats or using a software-based facilitating workflow with manual identification of the basal attachments points by using the software to place points with the subsequent position of the plane, or by a semiautomated software-based anatomical segmentation, which is verified by a trained observer and manual correction where required (6) (Fig 2c).

Multiple contouring tools exist for annular size quantification, including cubic spline interpolation, polygon tool, attenuation/Hounsfield unit-based contour detection, and freehand contour techniques (Fig 3). These tools give the annular area in either [mm2] or [cm2]. Smoothing algorithms are needed when using the latter techniques because these tools create irregular contours that falsely increase the annular perimeter. Most techniques give automatically short and long axis dimensions in [mm] using different methods that give information on the eccentricity of the annular cross-sectional dimensions and are better than manual caliper measurements when assessing the overall annular size (6).

While drawing the annular contour, no tissue should be seen within the contour and no contrast should be seen outside it and should be drawn in harmonic fashion irrespective of the presence of calcification (6). A double-oblique annular plane is necessary to achieve accurate measurements of aortic annulus (5). The annular area varies with the cardiac cycle phase, being larger during systole (22, 29). Hence, annular size quantification should be performed by choosing the reconstruction phase which yields the largest annular dimension with adequate image quality to avoid annular under-sizing (6). Sufficient contrast attenuation, absence of motion artifacts, and double contours are subjective criteria that can be used to assess image quality (6).

The annular area and perimeter are essential to determine the sizing of balloon-expandable devices and for self-expandable devices application respectively (6). It has been shown that annular measurements based on short and long-axis diameters are less reproducible than area or perimeter derived diameter and basal ring average diameter (30). Oversizing occurs when the native annulus is smaller than the deployed valve and it is measured as a percentage [%]: Oversizing [%] = (Valve nominal measurement/annular measurement − 1) × 100 (6).

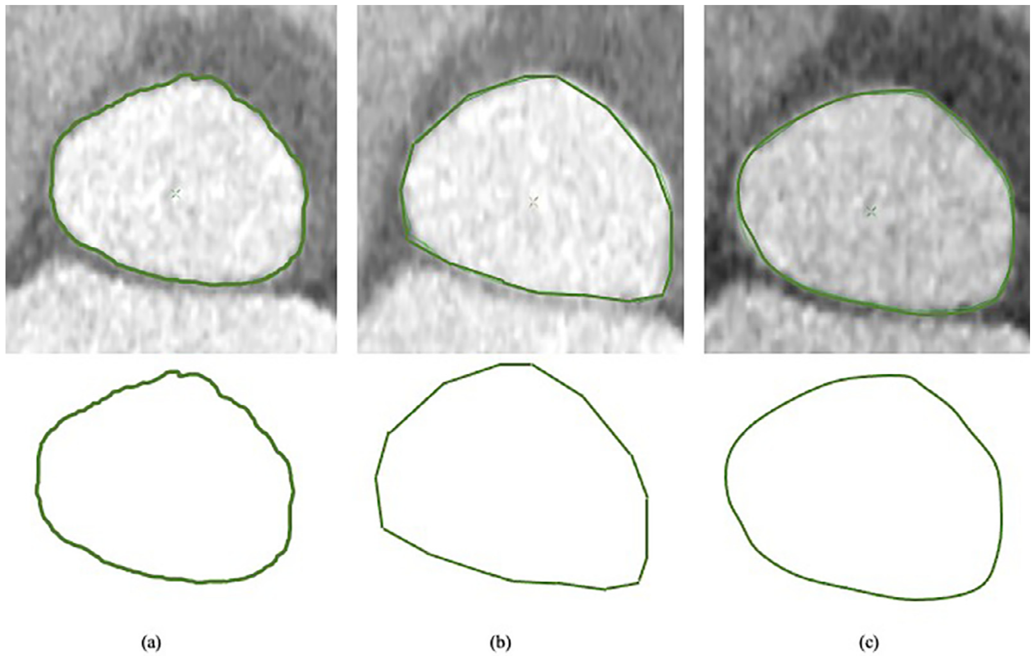

Figure 3. demonstrates the different contouring tools for computed tomography annular segmentation which include (a) the freehand tool which allows the drawing of a non-smooth irregular line around the aortic annulus, (b) the polygon tool which allows the manual placement of points around the aortic annulus which are then connected by straight lines and (c) the spline interpolation tool which prompts the manual placement of points which are connected by cubic spline interpolation.

Annular oversizing (especially with $>20\%$ oversizing) may increase the risk of annular rupture in presence of protruding landing zone calcification, particularly when present below the non-coronary cusp (31, 32). Other risk factors for annular rupture are female sex, use of balloon-expandable valves, and prior radiation therapy (6).

Magnetic Resonance Angiography (MRA)

Interestingly, cardiac gated 3D non-contrast-enhanced magnetic resonance angiography provides accurate aortic annulus measurement with low variability which correlates well with CTA measurements. This has made MRA an alternative imaging modality in patients where CTA is contraindicated (contrast media allergy, renal disease) and echocardiography when acoustic windows are restricted. Major limitations of MRA are inadequacy for imaging patients with metallic devices, claustrophobia, and its longer acquisition time (1, 33).

Aortic Valve Morphology

Calcification

The device landing zone is formed by the aortic annulus, the valvular cusps, and the LVOT (up to the junction point of the anterior mitral leaflet) (34). Calcification in the aortic complex is of special concern to radiologists and/or cardiologists since severe calcification within the LVOT and aortic valve increases the risk of paravalvular regurgitation (35). Therefore, it is essential to obtain an adequate description of the annular (within the annular plane) and sub-annular (upper 4 to 5 mm of the LVOT where the device gets into contact) calcium deposition. Calcification can be assessed qualitatively by echocardiography and CCT. In addition, CCT provides the ability to quantitatively assess the calcium burden using the Agatston method (17).

Qualitative Calcification Assessment by Echocardiography or CT (5):

- Presence of calcification: absent, mild, moderate, and severe.
- Number of calcifications: single and multiple.
- Extend of calcification: Symmetrical, asymmetrical, and circumferential.
- Position of Calcification: Annular or sub annular.
- The thickness of calcification: Linear or nodule-like.
- The aspect of calcification: Crescent, flat, adherent, protruding, and involving the cusps.

Quantitative Calcification Assessment by CT - Agatston method (5):

- Severe AS is very likely considered when Agatston scores are ≥ 3000 for men and ≥ 1600 for women.
- Severe AS is likely considered when Agatston scores are ≥ 2000 for men and ≥ 1200 for women.
- Severe AS is unlikely considered when Agatston scores are < 1600 for men and < 800 for women.

Cuspidity of Aortic Valve

Echocardiography is employed to differentiate tricuspid and bicuspid aortic valves (7,12). Bicuspid aortic valve appears as a fish-mouth (2 commissures) valve opening with closed raphe whereas a tricuspid aortic valve appears as an immobile tri-

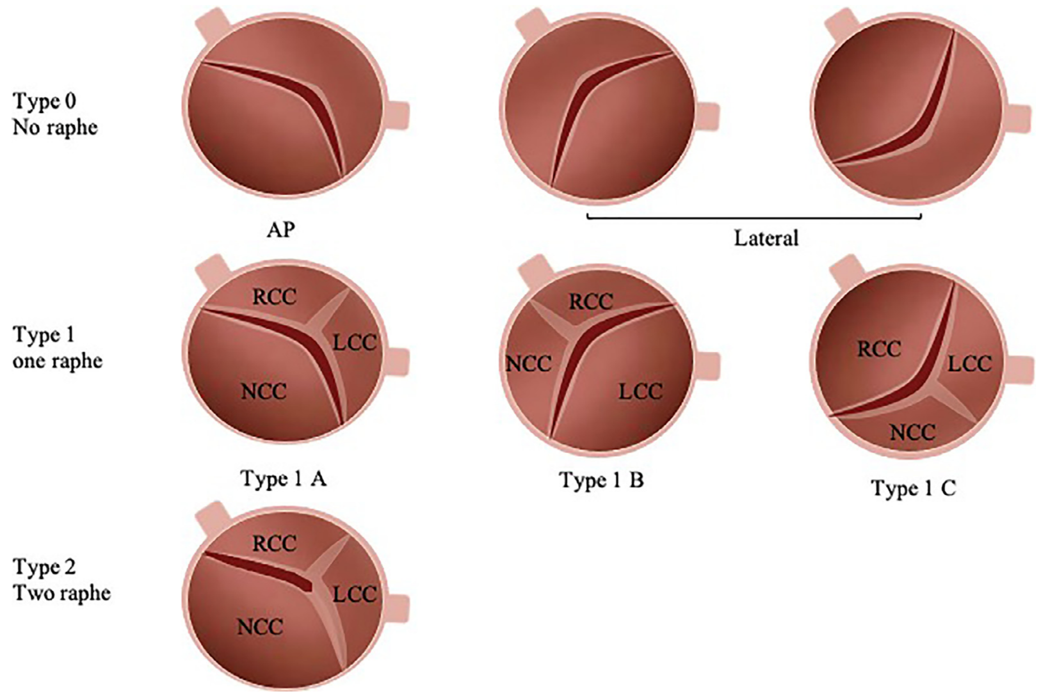

Figure 4. shows the schematic drawing of the bicuspid aortic valve Sievers classification which characterizes the valve according to the number of raphes where (a) Type 0 has no raphe (b) Type 1 has one raphe and (c) Type 2 has two raphes.

leaflet valve with flow in all three commissures. TTE has high sensitivity and specificity for bicuspid aortic valve diagnosis in valves with no or minimal calcification. However, in the case of heavily calcified valve, color TEE and CT are preferred over TTE (7,12).

The rate of bicuspid aortic valve (BAV) in patients presenting for TAVR may reach up to 6 % (36). A lower device success rate and a higher risk of paravalvular regurgitation occur in presence of BAV (37). There are several classifications of BAV morphology with Sievers classification being one of the most commonly used (38) which describes three different types according to the number of raphes (Figure 4): type 0 consists of valves with no raphes, type 1 with one raphe, and type 2 with 2 raphes. In the latter type, two hinge points exist to determine the annular size, for which a specific measurement technique is used (6). Ascending aortic dilation and aneurysms are more commonly seen in the bicommissural morphology. Description of raphe length and degree of calcification is essential since a higher risk of paravalvular regurgitation and rupture was seen with severe raphe calcification (37, 39).

Coronary Ostial Height and Sinus of Valsalva Assessment

It is important to measure the coronary height prior to TAVR procedure since a short coronary ostial height is associated with an increased risk of periprocedural coronary occlusion (5). This occurs due to the occlusion of the coronary ostium by displaced calcified coronary cusps. This risk should be assessed on CT by measuring the coronal ostial height from the annulus and the mean diameter of the sinus of Valsalva which predicts a higher risk of coronary occlusion if measure <10 mm and <30 mm, respectively with a narrow STJ (40).

The coronary ostial height should be measured in a perpendicular fashion to the annular plane using an electronic caliper tool from the annular plane to the lower edge of the coronary artery ostium (Figure 5). The sinus of Valsalva diameter should be measured cusp to commissure in parallel to the annular plane using three caliper measurements. For symmetric sinus of Valsalva anatomies, the three values can be averaged (6).

Sinotubular Junction and Ascending Aorta

The sinotubular junction (STJ) height should be measured in a perpendicular fashion to the annular plane using an electronic caliper tool from the annular plane to the lowest edge of the STJ, producing value in [mm]. STJ diameter should be measured using a caliper tool on an imaging plane aligned with the STJ. An STJ diameter smaller than the transcatheter heart valve predicts a higher risk of STJ injury in the case of balloon-expandable devices with low STJ height and calcification. Ascending aortic pathology should be evaluated and measured on double-oblique multiplanar reformats in [mm], either at the level of the greatest width or at the level of the main pulmonary artery (6).

VASCULAR ACCESS PLANNING

CT is recommended universally to assess vascular access during the pre-TAVR procedure. Vascular complications

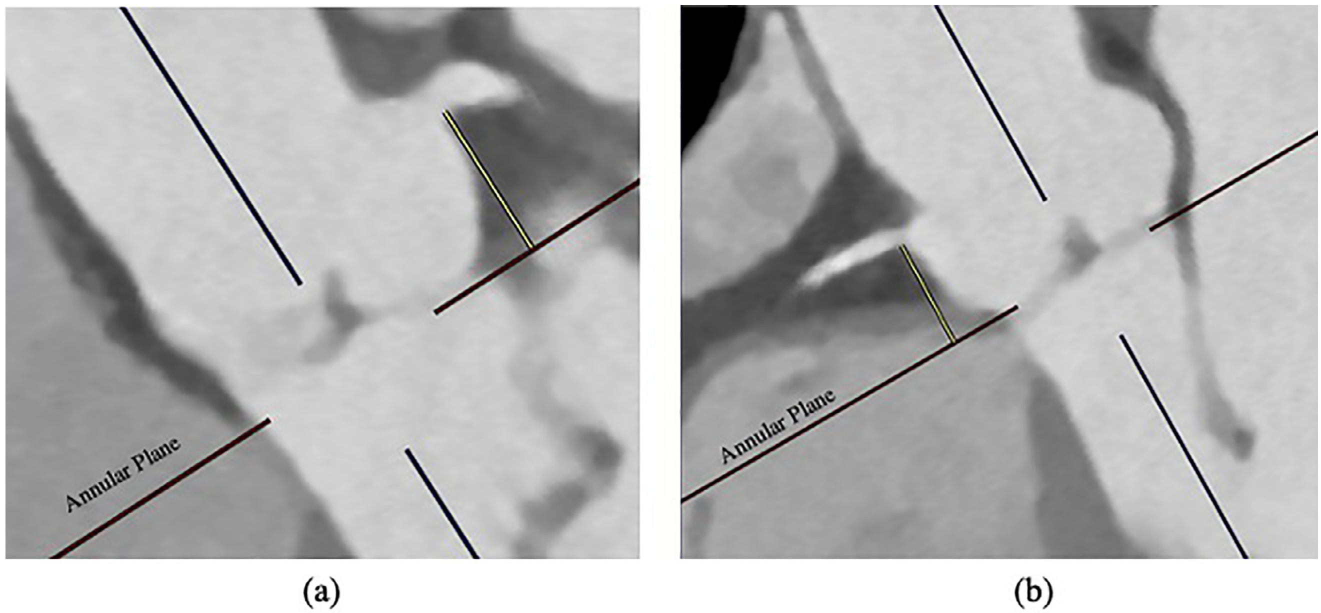

Figure 5. illustrates the sagittal computed tomography of the aortic complex demonstrating the (a) left coronary ostial height (yellow line) measured from the lower edge of the left coronary artery ostium to the annular plane perpendicularly and (b) the right coronary ostial height (yellow line) measured from the lower edge of the right coronary artery ostium to the annular plane perpendicularly.

account for 2-30% of all TAVR-related complications. Therefore, a comprehensive assessment of vascular access anatomy, size, patency, tortuosity, and presence of calcification is essential. This is most commonly performed with contrast-enhanced CT or MRI.

Non-ECG synchronized CTA of the aorto/ilio/femoral vasculature: It helps in choosing adequate vascular access, which is most commonly the common femoral artery. The scan coverage should include the aorta, iliac arteries, and common femoral arteries by extending from the upper thoracic aperture to the lesser trochanter (6, 41). The axial data set reconstruction for vascular access assessment should be obtained with ≤1.5 mm slice thickness, a large field of view, and either filtered back projection or iterative reconstruction.

There are multiple approaches for TAVR access. The transfemoral approach accounts for almost 90% of all TAVR procedures whereas transapical, aortic, axillary, and other approaches account for the remaining 10%.

Transfemoral Approach

Studies have shown that transfemoral vascular access has higher success and lower mortality rate compared to other vascular approaches.

CTA is the gold standard image modality for the assessment of vascular access in the pre-TAVR stage. For the iliofemoral approach, it is important to assess the arterial caliber (it should be at least 5.5 mm with 6.5 mm being ideally for an 18F delivery system), vascular angulation (>90 degree is generally problematic), presence of calcification (eccentric calcifications is not a problem whereas concentric calcification anywhere between the aortoiliac bifurcation to femoral arteries is problematic) and atherosclerotic burden (42). Additionally, a good assessment for the presence of aortic artery aneurysm, tortuosity, and thrombotic lesions should be performed since this could lead to an increased risk of complications when manipulating large catheters (2).

When CTA is contraindicated, unenhanced CMR can be performed. It provides a good correlation with CT in terms of aortic annulus and aortoiliofemoral diameter measurements (2). However, one of the major limitations of CMR, in this case, is its inability to detect calcifications that directly influence the vascular approach. Gadolinium-enhanced MRA can be employed for the assessment of vascular access (2, 33). Also, CMR using proton density-weighted in-phase stack of stars technique (PDIP-SOS) could be used for the assessment of aorto-iliac calcifications as multiples studies demonstrated its great correlation with CTA (43, 44).

Transaxillary Approach

In many hospitals, the transaxillary approach is considered the second most commonly employed vascular access after transfemoral. Similarly, to the transfemoral approach, the vascular caliber (>6.5 mm), presence of calcifications, tortuosity and angulation should be taken into consideration pre-TAVR. Interestingly, this vascular access was shown to match well with transfemoral access in terms of procedure success, vascular complications, and a 2-year survival rate albeit with a slight increase in stroke risk (42). Transaxillary access is not recommended for patients with short axillary arteries or significant tortuosity (2).

Transaortic Approach

This approach utilizes an upper ministernotomy to access the aorta. In this approach, it is important to assess the angulation of the aorta where a horizontal ascending aorta (>70° angulation) has a higher risk of valve malalignment. This approach can be safely employed in patients with lung diseases or low ejection fraction (2). Few contraindications include the presence of a short ascending aorta, porcelain aorta, and patients with previous bypass graft surgery with proximal anastomosis on the ascending aorta (42).

Transapical Approach

This approach involves puncturing the left ventricular apex after rib retraction and passage through the left pleural cavity. It accounts only for 1% of TAVR procedures and is the only approach that is anterograde and avoids cardiopulmonary bypass and sternotomy (2). Hemostasis issues may arise in a fragile ventricle and scarring can further reduce the left ventricular ejection fraction in patients with LV dysfunction. Contraindications include patients with advanced lung disease, low ejection fraction and left ventricular aneurysm (2).

Transcarotid Approach

It is one of the most common approaches employed in patients with multiple vascular diseases. It provides a direct and short route for accessing the aortic annulus. Transcarotid approach has an increased risk of ischemic brain injury prompting extensive imaging of the carotid artery and cerebral circulation prior to TAVR to assess its suitability. This is done with carotid duplex ultrasound, head CT, and brain MRA. The transcarotid approach is associated with minimal to no paravalvular leak, short hospital stay, early ambulation post-procedure, and minimal bleeding. Contraindications for this approach are patients with carotid artery diameter of > 8 mm or severe tortuosity (2).

OPTIMAL PROJECTION CURVE

CT scan can predict the appropriate C-arm position required for TAVR which is performed with specific fluoroscopic projection angulations (45), providing that patient's chest is positioned similarly on the CT table as during the procedure (6). These angulations optimize the initial pre-deployment fluoroscopic angulation with a reduction of radiation exposure, contrast usage, and procedural time (45). Typical views are either the 3 cusps view or cusps overlap view (6).

In patients with renal failure or iodinated contrast medium allergy, MRI can be an effective substitute to CT during the pre-TAVR planning phase, keeping in mind that MRI needs a longer acquisition time and requires patient cooperation.

PERI-TAVR IMAGING

Procedure Imaging

TAVR procedure is performed under sedation with fluoroscopic imaging which provides real-time monitoring and guidance of transcatheter navigation. It is majorly employed in conjunction with echocardiographic imaging which helps assess for immediate peri-TAVR complications such as tamponade, pericardial effusion, coronary occlusion, aortic dissection, aortic regurgitation (AR), and mitral regurgitation (MR) (41). TEE was the initial image modality used in TAVR intraprocedural guidance, but recent data showed a significant reduction in its application (from 60.7% in early TAVR 2 registry to 32.3% in later FRANCE TAVR data) (41). Furthermore, this was associated with a significant drop in in-hospital and 30-day mortality rates. Although TEE provides better visualization of structures and is associated with less incidence of acute kidney injury, physicians are substituting it with TTE due to its less invasive nature, no need for general anesthesia, and its association with shorter TAVR procedure time (8). The selection between TTE or TEE should be individualized according to the patient's specific condition.

Fusion imaging with EchoNavigator technology (Philips Medical System, Best, the Netherlands) provides patient-specific imaging by fusing fluoroscopic and TEE volumetric imaging data. This technology facilitates the manipulation and guidance of the prosthetic valve during TAVR and helps cardiologists to find the most suitable position for prosthetic valve deployment. CT does not play a role in peri-TAVR imaging (41).

Immediate Complications

Immediately after valve deployment, echocardiography is used to assess valve positioning, shape, leaflet motion, valvular mean pressure gradient, maximal velocity, and effective orifice area. Additionally, it provides a means to assess for immediate life-threatening TAVR complications (8).

Coronary Ostia Obstruction

It is important to visualize the coronary ostia and assess its flow by TEE and color doppler after prosthetic valve deployment to rule out eventual coronary ostial obstruction. Coronary obstruction is a rare life-threatening TAVR complication most commonly affecting females. It has an incidence of 0.66% and a one-year cumulative mortality rate of 45.5%. This complication can occur seconds to minutes from prosthetic valve deployment or after hours to years following insertion (46). Patients with a coronary ostial height CT measurement of <10 mm and mean diameter of the sinus of Valsalva <30 mm, are at increased risk of developing coronary obstruction post-TAVR (40). Coronary obstruction can also result in ventricular wall motion abnormalities and dysfunction (11).

Recent techniques have emerged to prevent coronary ostia obstruction mainly coronary protection technique and bioprosthetic or native aortic scallop intentional laceration to prevent iatrogenic coronary artery obstruction (BASILICA) procedure (47, 48). The coronary protection technique is employed post-TAVR in cases where there is impairment of coronary blood flow by wiring the coronary ostia with stent implantation (48). The BASILICA is a novel transcatheter technique employed immediately pre TAVR where the aortic leaflet is lacerated and split in two using radiofrequency from guidewire and is pushed aside during TAVR to maintain coronary artery blood flow preventing coronary ostial obstruction (47).

Aortic Root and Ascending Aorta Rupture and Dissection

It is a rare and life-threatening condition in which physicians should keep a low suspicion threshold in patients with rapid clinical deterioration. The incidence of aortic dissection accounts for 0.2 to 0.3% of all TAVR complications. It occurs during TAVR deployment possibly due to aortic damage from guidewire, mispositioning of the valve, or following balloon dilatation. If suspected, unenhanced CT is employed to assess for intramural hematoma, and then contrast-enhanced gated CT is performed for the evaluation of the dissection flap (46).

Mitral Valve Injury or Mitral Regurgitation

Mitral regurgitation can occur due to valvular injury or rupture chordae tendinea while manipulating the wire when entering the left ventricle.

Transvalvular and Paravalvular Aortic Regurgitation (AR)

Its incidence is associated with increased short and long-term mortality rates in TAVR patients. Transvalvular AR occurs due to the employment of stiff wires across the aortic valve (11). Most transvalvular AR cases are resolved after the removal of the TAVR procedural wire. Paravalvular regurgitation occurs due to inadequate prosthetic valve apposition to the annulus secondary to heavy calcifications (on the device landing zone) and under-sizing, or malposition of prosthetic valve (46). Unfortunately, paravalvular AR impacts negatively TAVR's long-term prognosis with even mild paravalvular regurgitation being associated with an increased mortality rate (46). Doppler echocardiography, mainly through a parasternal short-axis approach, is employed to assess and grade paravalvular AR, where the circumferential burden of paravalvular jets classifies it as mild (<10%), moderate (10-29%), and severe (>= 30%) (46). Additionally, CMR can effectively detect paravalvular regurgitation due to its phase-contrast sequences which provide flow measurements in the aorta (49). In cases of paravalvular regurgitation, balloon dilatation, plug insertion or a new prosthetic valve deployment may be required (11).

Pericardial Effusion and Tamponade

Pericardial effusion and tamponade should be suspected in patients in the setting of hypotension. Perforation from the RV can usually be managed by pericardiocentesis, in contrast to an LV perforation that necessitates an emergent surgical intervention and is associated with high mortality rates (11).

Valve Migration and Embolization

It is a rare complication that accounts for less than 1% of all TAVR complications in Corevalve and 0.2% in Evolut R valve (49). It occurs within 60 minutes of valve deployment and results from malpositioning of the prosthetic valve leading to its complete displacement from its original implanted position reaching the aorta or left ventricle (46). Patients with aortic root angulation and asymmetrical calcifications of the aortic valve are at increased risk of developing this adverse event (46).

Annular Rupture

Aortic annular rupture accounts for 1% of all TAVR complications. It is classified according to its location (intra-annular, sub-annular, or supra-annular) (46). It occurs due to inaccurate measurements of the aortic annulus area leading to prosthetic valve oversizing. Additionally, failure of detection of LVOT calcification may result in aortic annular rupture (49). Clinically patients may become hemodynamically unstable due to the development of cardiac tamponade or may present with AV fistula, septal defects, and intraluminal hematomas.

POST-TAVR IMAGING

Postprocedural follow-up is employed to evaluate structural valve status and post-TAVR complications. TTE is the main image modality employed to assess valve function. According to the Valve Academic Research Consortium (VARC)-2, follow-up TTE is recommended at one, six, and 12 months post TAVR procedure and yearly thereafter (11). Additionally, it should always be performed in TAVR patients who develop a new-onset murmur or symptoms of heart failure (11). There is no consensus for the employment of routine CCT imaging post-TAVR unless a complication is suspected or detected through TTE (6). CCT is employed in conjunction with echocardiography when there is high suspicion for infective endocarditis, valve thrombosis, structural degeneration, and when patient is hemodynamically unstable.

1. Stent fracture

It is an extremely rare complication mainly detected by the presence of an indentation or discontinuation of the metallic structure of the prosthetic valve by CT (46).

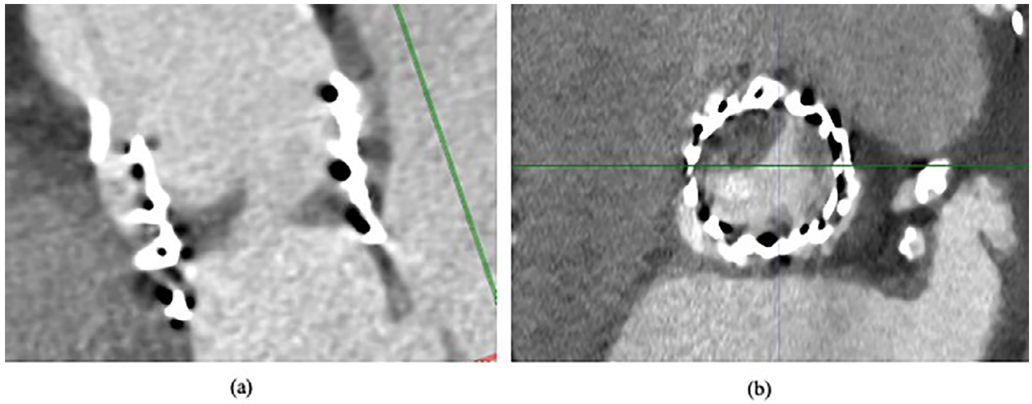

Figure 6. CT Angiography showing hypoattenuating leaflet thickening involving >50% of the aortic prosthesis, consistent with leaflet thrombosis. Patient had TAVR three years ago and presented with increasing dyspnea at minimal exertion.

2. Valve Thrombosis

Valve thrombosis is a relatively common late complication of TAVR, characterized by a significant increase in doppler aortic valve gradient (increase in the mean gradient of ≥10 mm Hg over time) (46). Once this is detected, an ECG-gated CT is recommended due to its high spatial resolution and minimal artifact from the metallic stent (49). CT imaging of the prosthetic valve will show crescent-shaped hypoattenuated leaflets thickening (HALT) with reduced leaflet motion (RLM) and filling defects in the valvular cusps (Fig 6) (46).

The extent of HALT and RLM can be graded by 4D-CT imaging into (50):

Grade 0: No HALT and RLM.
Grade 1: ≤ 25% HALT or RLM.
Grade 2: 26-50% HALT or RLM.
Grade 3: 51-75% HALT or RLM.
Grade 4: >75% HALT or RLM.

3. Conduction Disturbances

Conduction disturbance is a common post-TAVR complication. It is associated with increased hospitalization and mortality rates (46). Atrioventricular block may occur due to the close relationship between the device landing zone and the conduction system and warrants pacemaker insertion, particularly in the presence of severe sub-annular calcification and pre-existent right bundle branch block (51). It is estimated that almost 6-20% of patients require pacemaker implantation post-TAVR (46).

Left bundle branch block risk is higher with increased depth of implantation post-TAVR using balloon- or self-expandable prostheses (52, 53). An associated deep implant depth or pre-existent right bundle branch block and short semi-membranous septum, less than 8 cm, increases the risk of conduction abnormalities (54, 55).

4. Prosthesis-Patient Mismatch

It results from the mismatch in effective orifice area (EOA) of the prosthetic device compared to the patient's body size, where the former is too small in relation to the latter. It is less common in TAVR procedures compared to SAVR. It is diagnosed by using the EOA index to body surface (EOAi) where it is absent if EOAi >0.85 cm2/m2, moderate if 0.65≤ EOAi <0.85 cm2/m2 and severe if EOAi<0.65 cm2/m2.

5. Infective Endocarditis

It is a life-threatening complication that may occur around 6 months post-TAVR.

CONCLUSION

TAVR has become the standard procedure for managing patients with moderate to severe AS. Imaging plays a crucial role in pre, peri, and post TAVR procedure. In the pre-TAVR stage, CT and echocardiography provide the ability to assess AS severity, patient's suitability to TAVR, and determine prosthetic valve sizing which is essential for a successful TAVR procedure. Furthermore, echocardiography provides real-time guidance during the procedure and the ability to evaluate for early and late complications. Multi-image modalities may be employed in each stage for the achievement of optimal guidance due to the complexity and confounding structural and functional cardiac conditions.

REFERENCES

1. Leipsic JA, Blanke P, Hanley M, et al. ACR appropriateness criteria® imaging for transcatheter aortic valve replacement. J Am College of Radiol 2017; 14(11):S449–S455.
2. Pour-Ghaz I, Raja J, Bayoumi M, et al. Transcatheter aortic valve replacement with a focus on transcarotid: a review of the current literature. Ann translational med 2019; 7(17):420.

3. Scully PR, Patel KP, Treibel TA, et al. Prevalence and outcome of dual aortic stenosis and cardiac amyloid pathology in patients referred for transcatheter aortic valve implantation. Eur Heart J 2020; 41(29):2759–2767.
4. Randall MH, Bavry AA. Update on transcatheter aortic valve replacement. Cardiol and Therapy 2020: 1–10.
5. Grutta LLa, Toia P, Grassedonio E, et al. TAVI imaging: over the echocardiography. La radiologia medica 2020; 125(11):1148–1166.
6. Blanke P, Weir-McCall JR, Achenbach S, et al. Computed tomography imaging in the context of transcatheter aortic valve implantation (TAVI)/transcatheter aortic valve replacement (TAVR): An expert consensus document of the Society of Cardiovascular Computed Tomography. JACC: Cardiovascular Imaging 2019; 12(1):1–24.
7. Vollema EM, Delgado V, Bax JJ. Echocardiography in transcatheter aortic valve replacement. Heart, Lung and Circulation 2019; 28(9):1384–1399.
8. Liu Q, Hahn RT. The role of multimodality imaging in transcatheter aortic valve replacement. Current Cardiol Rep 2019; 21(8):84.
9. Veulemans V, Afzal S, Papadopoulos G, et al. TAVR-related echocardiographic assessment−status quo, challenges and perspectives. Acta Cardiologica 2019: 1–11.
10. M. Dania Mohty, PhD, Clinical manifestations and diagnosis of low gradient severe aortic stenosis, 2020. https://www.uptodate.com/contents/clinical-manifestations-and-diagnosis-of-low-gradient-severe-aortic-stenosis. Last accessed 9 August 2021.
11. Onishi T, Sengoku K, Ichibori Y, et al. The role of echocardiography in transcatheter aortic valve implantation. Cardiovasc diagnosis and therapy 2018; 8(1):3.
12. Hahn RT, Nicoara A, Kapadia S, et al. Echocardiographic imaging for transcatheter aortic valve replacement. J Am Soc Echocardiography 2018; 31(4):405–433.
13. Clavel M-A, Malouf J, Messika-Zeitoun D, et al. Aortic valve area calculation in aortic stenosis by CT and doppler echocardiography. JACC: Cardiovasc Imaging 2015; 8(3):248–257.
14. Alkadhi H, Leschka S, Trindade PT, et al. Cardiac CT for the differentiation of bicuspid and tricuspid aortic valves: comparison with echocardiography and surgery. Am J Roentgenol 2010; 195(4):900–908.
15. Bennett CJ, Maleszewski JJ, Araoz PA. CT and MR imaging of the aortic valve: radiologic-pathologic correlation. Radiographics 2012; 32 (5):1399–1420.
16. Baumgartner H, Falk V, Bax JJ, et al. 2017 ESC/EACTS guidelines for the management of valvular heart disease. Eur heart j 2017; 38(36):2739–2791.
17. Eberhard M, Hinzpeter R, Polacin M, et al. Reproducibility of aortic valve calcification scoring with computed tomography−an interplatform analysis. J cardiovasc computed tomography 2019; 13(2):92–98.
18. Clavel M-A, Messika-Zeitoun D, Pibarot P, et al. The complex nature of discordant severe calcified aortic valve disease grading: new insights from combined Doppler echocardiographic and computed tomographic study. J Am College of Cardiol 2013; 62(24):2329–2338.
19. Kim HJ, Choe YH, Kim SM, et al. A new method for aortic valve planimetry with high-resolution 3-dimensional MRI and its comparison with conventional cine mri and echocardiography for assessing the severity of aortic valvular stenosis. Korean J Radiol 2021; 22.
20. Piazza N, de Jaegere P, Schultz C, et al. Anatomy of the aortic valvar complex and its implications for transcatheter implantation of the aortic valve. Circulation: Cardiovasc Interventions 2008; 1(1):74–81.
21. Anderson RH. Clinical anatomy of the aortic root. Heart 2000; 84(6):670–673.
22. Sucha D, Tuncay V, Prakken NH, et al. Does the aortic annulus undergo conformational change throughout the cardiac cycle? A systematic review. Eur Heart J-Cardiovasc Imaging 2015; 16(12):1307–1317.
23. Jurencak T, Turek J, Kietselaer BL, et al. MDCT evaluation of aortic root and aortic valve prior to TAVI. What is the optimal imaging time point in the cardiac cycle? Eur radiol 2015; 25(7):1975–1983.
24. Willson AB, Webb JG, Freeman M, et al. Computed tomography−based sizing recommendations for transcatheter aortic valve replacement with balloon-expandable valves: Comparison with transesophageal echocardiography and rationale for implementation in a prospective trial. J cardiovasc computed tomography 2012; 6(6):406–414.
25. de Heer LM, Budde RP, van Prehn J, et al. Pulsatile distention of the nondiseased and stenotic aortic valve annulus: analysis with electrocardiogram-gated computed tomography. The Ann thoracic surg 2012; 93 (2):516–522.
26. Søndergaard L, Steinbrüchel DA, Ihlemann N, H., et al. Two-year outcomes in patients with severe aortic valve stenosis randomized to transcatheter versus surgical aortic valve replacement: the all-comers nordic aortic valve intervention randomized clinical trial. Circulation: Cardiovasc Interventions 2016; 9(6):e003665.
27. Tamburino C, Barbanti M, D'Errigo P, et al. 1-year outcomes after transfemoral transcatheter or surgical aortic valve replacement: results from the Italian OBSERVANT study. J Am College of Cardiol 2015; 66(7):804–812.
28. Abbara S, Blanke P, Maroules CD, et al. SCCT guidelines for the performance and acquisition of coronary computed tomographic angiography: a report of the society of Cardiovascular Computed Tomography Guidelines Committee: endorsed by the North American Society for Cardiovascular Imaging (NASCI). J cardiovasc computed tomography 2016; 10 (6):435–449.
29. Murphy DT, Blanke P, Alaamri S, et al. Dynamism of the aortic annulus: effect of diastolic versus systolic CT annular measurements on device selection in transcatheter aortic valve replacement (TAVR). J cardiovascular computed tomography 2016; 10(1):37–43.
30. Gurvitch R, Webb JG, Yuan R, et al. Aortic annulus diameter determination by multidetector computed tomography: reproducibility, applicability, and implications for transcatheter aortic valve implantation. JACC: Cardiovasc Interventions 2011; 4(11):1235–1245.
31. Hansson NC, Nørgaard BL, Barbanti M, et al. The impact of calcium volume and distribution in aortic root injury related to balloon-expandable transcatheter aortic valve replacement. J cardiovasc computed tomography 2015; 9(5):382–392.
32. Barbanti M, Yang T-H, Rodès Cabau J, et al. Anatomical and procedural features associated with aortic root rupture during balloon-expandable transcatheter aortic valve replacement. Circulation 2013; 128(3):244–253.
33. Toy D, Kallianos K. Beyond annulus size: imaging for TAVR Planning. Current Radiol Reports 2018; 6(12):48.
34. Latsios G, Gerckens U, Buellesfeld L, et al. Device landing zone" calcification, assessed by MSCT, as a predictive factor for pacemaker implantation after TAVI. Catheterization and cardiovasc interventions 2010; 76 (3):431–439.
35. Hansson NC, Leipsic J, Pugliese F, et al. Aortic valve and left ventricular outflow tract calcium volume and distribution in transcatheter aortic valve replacement: influence on the risk of significant paravalvular regurgitation. J cardiovasc computed tomography 2018; 12(4):290–297.
36. Yoon S-H, Ahn J-M, Hayashida K, et al. Clinical outcomes following transcatheter aortic valve replacement in Asian population. JACC: Cardiovasc Interventions 2016; 9(9):926–933.
37. Yoon S-H, Bleiziffer S, De Backer O, et al. Outcomes in transcatheter aortic valve replacement for bicuspid versus tricuspid aortic valve stenosis. J Am College of Cardiol 2017; 69(21):2579–2589.
38. Ridley CH, Vallabhajosyula P, Bavaria JE, et al. The Sievers classification of the bicuspid aortic valve for the perioperative echocardiographer: the importance of valve phenotype for aortic valve repair in the era of the functional aortic annulus. J cardiothoracic and vascular anesth 2016; 30 (4):1142–1151.
39. Jilaihawi H, Chen M, Webb J, et al. A bicuspid aortic valve imaging classification for the TAVR era. JACC: Cardiovasc Imaging 2016; 9(10):1145–1158.
40. Ribeiro HB, Webb JG, Makkar RR, et al. Predictive factors, management, and clinical outcomes of coronary obstruction following transcatheter aortic valve implantation: insights from a large multicenter registry. J Am College of Cardiol 2013; 62(17):1552–1562.
41. Bleakley C, Monaghan MJ. The pivotal role of imaging in TAVR Procedures. Current Cardiol Reports 2018; 20(2):9.
42. Biasco L, Ferrari E, Pedrazzini G, et al. Access sites for TAVI: patient selection criteria, technical aspects, and outcomes. Frontiers in cardiovasc med 2018; 5:88.
43. Serhal A, Koktzoglou I, Aouad P, et al. Cardiovascular magnetic resonance imaging of aorto-iliac and ilio-femoral vascular calcifications using proton density-weighted in-phase stack of stars. J Cardiovasc Magnetic Resonance 2018; 20(1):51.
44. Ferreira Botelho MP, Koktzoglou I, Collins JD, S., et al. MR imaging of iliofemoral peripheral vascular calcifications using proton density-weighted, in-phase three-dimensional stack-of-stars gradient echo. Magn Reson Med 2017; 77(6):2146–2152.
45. Samim M, Stella PR, Agostoni P, et al. Automated 3D analysis of pre-procedural MDCT to predict annulus plane angulation and C-arm positioning: benefit on procedural outcome in patients referred for TAVR. JACC: Cardiovasc Imaging 2013; 6(2):238–248.

46. Naik M, McNamara C, Jabbour RJ, et al. Imaging of transcatheter aortic valve replacement complications. Clin Radiol 2020.
47. Khan JM, Greenbaum AB, Babaliaros VC, et al. The BASILICA trial: prospective multicenter investigation of intentional leaflet laceration to prevent TAVR coronary obstruction. JACC: Cardiovasc Interventions 2019; 12(13):1240–1252.
48. Palmerini T, Chakravarty T, Saia F, et al. Coronary protection to prevent coronary obstruction during TAVR: a multicenter international registry. Cardiovasc Interventions 2020; 13(6):739–747.
49. Aung H, Williamson EE, Singh SP. Transcatheter aortic valve replacement: preprocedure and postprocedure imaging. Advances in Clin Radiol 2019; 1:119–134.
50. Blanke P, Leipsic JA, Popma JJ, et al. Bioprosthetic aortic valve leaflet thickening in the evolut low risk sub-study. J Am College of Cardiol 2020; 75(19):2430–2442.
51. Fujita B, Kütting M, Seiffert M, et al. Calcium distribution patterns of the aortic valve as a risk factor for the need of permanent pacemaker implantation after transcatheter aortic valve implantation. Eur J Echocardiography 2016; 17(12):1385–1393.
52. Urena M, Mok M, Serra V, et al. factors and long-term clinical consequences of persistent left bundle branch block following transcatheter aortic valve implantation with a balloon-expandable valve. J Am College of Cardiol 2012; 60(18):1743–1752.
53. Calvi V, Conti S, Pruiti GP, et al. Incidence rate and predictors of permanent pacemaker implantation after transcatheter aortic valve implantation with self-expanding CoreValve prosthesis. J interventional cardiac electrophysiol 2012; 34(2):189–195.
54. Maeno Y, Abramowitz Y, Kawamori H, et al. A highly predictive risk model for pacemaker implantation after TAVR. JACC: Cardiovasc Imaging 2017; 10(10):1139–1147. Part A.
55. Hamdan A, Guetta V, Klempfner R, et al. Inverse relationship between membranous septal length and the risk of atrioventricular block in patients undergoing transcatheter aortic valve implantation. JACC: Cardiovasc Interventions 2015; 8(9):1218–1228.